Materials Today Bio 22 (2023) 100769

Contents lists available at ScienceDirect

Materials Today Bio

journal homepage: www.journals.elsevier.com/materials-today-bio

Hydrogel degradation promotes angiogenic and regenerative potential of cell spheroids for wound healing

Victoria L. Thai [a,b], David H. Ramos-Rodriguez [a], Meron Mesfin [b], J. Kent Leach [a,b,*]

[a] Department of Orthopaedic Surgery, UC Davis Health, Sacramento, CA, 95817, USA
[b] Department of Biomedical Engineering, UC Davis, Davis, CA, 95616, USA

ARTICLE INFO

Keywords:
Spheroids
Mesenchymal stromal cell
Endothelial cell
poly(ethylene) glycol
Degradation

ABSTRACT

Chronic nonhealing wounds are debilitating and diminish one's quality of life, necessitating the development of improved strategies for effective treatment. Biomaterial- and cell-based therapies offer an alternative treatment compared to conventional wound care for regenerating damaged tissues. Cell-based approaches frequently utilize endothelial cells (ECs) to promote vascularization and mesenchymal stromal cells (MSCs) for their potent secretome that promotes host cell recruitment. Spheroids have improved therapeutic potential over monodisperse cells, while degradable scaffolds can influence cellular processes conducive to long-term tissue regeneration. However, the role of biomaterial degradation on the therapeutic potential of heterotypic EC-MSC spheroids for wound healing is largely unknown. We formed poly(ethylene) glycol (PEG) hydrogels with varying ratios of matrix metalloproteinase (MMP)-degradable and non-degradable crosslinkers to develop three distinct constructs – fully degradable, partially degradable, and non-degradable – and interrogate the influence of degradation rate on engineered cell carriers for wound healing. We found that the vulnerability to degradation was critical for cellular proliferation, while inhibition of degradation impaired spheroid metabolic activity. Higher concentrations of degradable crosslinker promoted robust cell spreading, outgrowth, and secretion of proangiogenic cytokines (*i.e.*, VEGF, HGF) that are critical in wound healing. The degree of degradation dictated the unique secretory profile of spheroids. When applied to a clinically relevant full-thickness *ex vivo* skin model, degradable spheroid-loaded hydrogels restored stratification of the epidermal layer, confirming the efficacy of scaffolds to promote wound healing. These results highlight the importance of matrix remodeling and its essential role in the therapeutic potential of heterotypic spheroids.

Statement of significance

Wound healing is dependent upon extracellular matrix (ECM) remodeling by matrix metalloproteinases (MMPs), while dysregulation can lead to chronic wounds. In this study, we used poly(ethylene) glycol (PEG) hydrogels formed with an MMP-degradable crosslinker (*i.e.*, GPQ-A) to interrogate the influence of degradation rate on engineered cell carriers for angiogenesis and wound healing. This study highlights the importance of rapid hydrogel degradation, achieved through endogenous MMP secretion by entrapped heterotypic spheroids, on cell sprouting, migration, proangiogenic growth factor production, and repair of an *ex vivo* full thickness wound. The results of these studies describe the influence of degradability on the regenerative potential of EC-MSC spheroids and confirm that the degradability of the cell carrier should be carefully considered.

1. Introduction

Wound healing is comprised of an intricate cascade of events – hemostasis, inflammation, proliferation, and maturation/remodeling. Impaired healing is prevalent in individuals who suffer from diabetes, cardiovascular diseases, renal disease, or obesity and can lead to the development of nonhealing chronic wounds [1,2]. Chronic wounds affect 6.5 million patients in the USA [3]. In 2022, the global chronic wound care market was $12.3 billion (USD) and is projected to be over $19 billion by 2029 [4]. Common treatments include topical wound medications/dressings and debridement, which maintains a moist environment and removes necrotic tissues to aid in granulation tissue formation. However, these approaches are limited because they do not address underlying vascularization impairments characteristic of full-thickness wounds. Alternative approaches such as cellular or

* Corresponding author. Department of Orthopaedic Surgery, UC Davis Health, 4860 Y St., Suite 3800, Sacramento, CA, 95817, USA.
E-mail address: jkleach@ucdavis.edu (J.K. Leach).

https://doi.org/10.1016/j.mtbio.2023.100769
Received 4 June 2023; Received in revised form 27 July 2023; Accepted 9 August 2023
Available online 11 August 2023

acellular dermal matrices have been utilized, but these matrices are restricted by their cost, donor availability, and donor site morbidity [5].

There is a critical need for the development of improved cell-based therapies to regenerate damaged tissues such as large skin wounds. Mesenchymal stromal cells (MSCs) are commonly used due to their bioactive secretome that modulates the recruitment of important host cells, while endothelial cells (ECs) are integral for their ability to directly form blood vessels to increase blood flow to the wound bed, respectively [6–9]. Spheroids, three-dimensional cellular aggregates, have attracted attention in the field of regenerative medicine as they possess increased cell viability in harsh microenvironments and secrete increased concentrations of endogenous trophic factors compared to monodisperse and monolayer counterparts [10]. Spheroids better mimic native tissues due to increased cell-to-cell interactions. Specifically, MSCs cultured as self-assembled 3D aggregates exhibited enhanced proliferation and metabolic reconfiguration, while ECs in spheroidal form displayed increased expressions of genes associated with cell survival and proliferation [11–13]. We explored the communication between ECs and MSCs to improve network formation and recently reported that the culture microenvironment can potentiate the angiogenic and re-epithelialization potentials of EC-MSC spheroids [14,15]. Furthermore, incorporating ECs into MSC spheroids enhanced the angiogenic potential [16]. Due to the advantages of co-culturing ECs and MSCs, we leveraged these two cell types in these studies.

In addition to cell-based therapies, hydrogels composed of natural (*e.g.*, alginate and collagen) and synthetic (*e.g.*, poly(ethylene glycol) (PEG)) polymers have been employed as cell and drug delivery carriers or dressings to promote skin repair. During dermal wound healing, proteolytic enzymes including matrix metalloproteinases (MMPs) regulate inflammation to induce migration of host cells (*i.e.*, ECs, fibroblasts, keratinocytes) by degrading and remodeling the wound ECM [17]. However, chronic wounds are marked by excessive protease activity [17,18]. Degradable hydrogels represent an emerging platform used to modulate extracellular matrix (ECM) remodeling for enhanced cell migration, macrophage polarization to a pro-regenerative phenotype, neovascularization, and collagen deposition for wound repair [19–25]. PEG-based hydrogels are widely used due to their biocompatibility, hydrophilicity, and tunability [26]. For instance, 4-arm PEG-maleimide (PEG-4MAL) macromer has been extensively investigated and tuned to achieve varying rates of degradation by using different crosslinkers, which influenced the physical and chemical properties of the hydrogel [22,27–29]. While the development of PEG-4MAL hydrogels with varying rates of degradation is well-characterized, the influence of matrix degradation rate on the therapeutic potential of co-culture EC-MSC spheroids for wound healing remains largely unknown.

In this study, we investigated the role of microenvironmental degradation on the therapeutic potential of EC-MSC spheroids when delivered in a highly biocompatible, tunable, and well-characterized degradable PEG-based hydrogel. We hypothesized that the degradability of the biomaterial cell carrier would regulate cell outgrowth and cytokine production by EC-MSC spheroids and modulate tissue regeneration. This study highlights the importance of matrix remodeling on the therapeutic potential of EC-MSC spheroids and illustrates the utility of tuning scaffold degradability to potentiate their efficacy when used as cell carriers for wound healing.

2. Materials and methods

2.1. Cell culture and spheroid formation

Human endothelial colony-forming cells (ECs) were isolated from human cord blood obtained through the UC Davis Cord Blood Collection Program (UCBCP) [30], and a subset of cells were modified to express green fluorescent protein (GFP) as described [14]. ECs were expanded in EGM-2 supplemented media (PromoCell, Heidelberg, Germany) with gentamicin (50 μg/mL; ThermoFisher, Waltham, MA) and amphotericin B (50 ng/mL; ThermoFisher) under standard culture conditions (37°C, 5% CO_2, 21% O_2) until use at passages 7–8. Media changes were performed every 2 days. Human bone marrow-derived MSCs from a single donor (RoosterBio, Inc., Frederick, MD) were expanded without further characterization in standard culture conditions in minimum essential alpha medium (α-MEM; Invitrogen, Carlsbad, CA) supplemented with 10% fetal bovine serum (FBS; Atlanta Biologicals, Flowery Branch, GA) and 1% penicillin/streptomycin (P/S; Gemini Bio-Products, Sacramento, CA) until use at passages 4–5. Media changes were performed every 2–3 days.

Co-culture EC-MSC spheroids were formed using a forced aggregation method [31]. Briefly, ECs and MSCs were pipetted into 1.5% agarose molds in well plates to produce spheroids of 15,000 cells (5000 ECs and 10,000 MSCs), and the plates were centrifuged at 500×*g* for 8 min. Spheroid size and ratio of cell types were chosen based on prior data exhibiting robust vasculogenic potential of EC-MSC spheroids [15,32]. Plates were maintained in static culture conditions (37°C, 5% CO_2, 21% O_2) for 48 h in 3:1 EGM-2:α-MEM (3:1 media) for spheroid formation.

2.2. PEG-4MAL hydrogel synthesis and spheroid encapsulation

We fabricated protease-cleavable or non-degradable hydrogels as previously described [33]. Briefly, four-arm poly(ethylene glycol) (PEG) macromer with maleimide groups at each terminus (PEG-4MAL) (MW 20,000; Laysan Bio, Arab, AL) was dissolved in 4-(2-hydroxyethyl)-1-piperazineethanesulfonic acid) (HEPES) buffer (20 mM in DPBS, pH 7.4). Adhesive peptide (GRGDSPC, RGD-C, pH 5.5–6; GenScript, Piscataway, NJ) was dissolved in HEPES to generate the functionalized PEG-4MAL precursor. Bis-cysteine cross-linking peptide GCRDGPQG↓IAGQDRCG (GPQ-A, ↓ denotes enzymatic cleavage site, pH 4.5 ± 0.1; GenScript) and poly(ethylene) glycol dithiol (PEG-DT, MW 5000, pH 4.5 ± 0.1; JenKem Technology, Plano, TX) were dissolved in HEPES at 1:1 maleimide/cysteine ratio after accounting for maleimide groups reacted with adhesive peptide. RGD-C was polymerized to PEG-4MAL macromer at 37°C for at least 15 min. Spheroid suspensions were added to the functionalized PEG-4MAL precursor to achieve a final concentration of 3×10^6 cells/mL. Gels were individually synthesized by mixing the PEG-4MAL solution with varying ratios of GPQ-A and PEG-DT in 8 mm diameter circular silicone molds to achieve completely degradable gels (100% GPQ-A (GPQ-A)), partially degradable gels (50% GPQ-A and 50% PEG-DT (GPQ-A:PEG-DT)), or non-degradable gels (100% PEG-DT (PEG-DT)) [15,33]. Hydrogels were crosslinked at 37°C for 20 min to produce 8.0% 20-kDa PEG-4MAL (wt/vol) hydrogels with a final adhesive ligand concentration of 2 mM. Following gelation, the gels were transferred into individual wells of 24-well plates, and the 3:1 medium was refreshed every 2 days. Media from spheroid-entrapped gels was refreshed (1 mL) 24 h prior to collection as conditioned media (CM).

2.3. Mechanical and degradation characterization of PEG-4MAL hydrogel

PEG-4MAL gels were allowed to swell for 24 h in α-MEM prior to analysis using a Discovery HR2 Hybrid Rheometer (TA Instruments, New Castle, DE) using a stainless steel, cross-hatched, 8 mm plate geometry. Before rheological testing, the gels were cut to fit the plate geometry using a biopsy punch. We determined storage moduli by performing an oscillatory frequency sweep ranging from 0.1 to 100 rad s^{-1} at a strain of 0.5% on each gel to obtain the linear elastic region before gel failure. At least five data points were collected for the linear elastic region and averaged to obtain gel shear storage modulus. Gels were measured after 1 and 7 days in fully supplemented α-MEM at 37°C. Prior to mechanical testing on days 1 and 7, the wet mass of the gels was obtained using a Mettler Toledo XPR2 Microbalance (Mettler-Toledo,

Columbus, OH). After testing, gels were frozen and lyophilized for 24 h or until dry before measuring the dry mass. Gross morphological images were taken of the gels following formation and 24 h swelling.

To investigate the contribution of spheroids on PEG-4MAL gel degradation, we measured the storage moduli, wet mass, and dry mass on days 1 and 7 post-spheroid encapsulation. Some gels were treated with GM6001 (25 μM; Sigma-Aldrich, St. Louis, MO), a broad-spectrum MMP inhibitor, to limit GPQ-A crosslinker cleavage from MMP-2 activity and impede hydrogel degradation [34].

2.4. EC-MSC spheroid response to degradable PEG-4MAL gels

We assessed cell viability by a Live/Dead assay per the manufacturer's protocol (Thermo Fisher), and metabolic activity was determined using an alamarBlue assay (Invitrogen) with fluorescence read at 590 nm. DNA content was measured *via* PicoGreen dsDNA assay (Invitrogen). After 1 and 7 days in culture, spheroids were imaged *via* brightfield microscopy to determine cell spreading. We evaluated cell spreading from spheroids in ImageJ (NIH) by quantifying the number of protrusions from the spheroids and the protrusion lengths by measuring from the center of the spheroid to the leading edge in the z-plane where the spheroid diameter was maximal. We used a threshold of 12 μm to determine cell spreading based on the cellular dimensions of ECs and MSCs [35,36]. At least three representative sprouts were captured per spheroid, and at least three spheroids were measured per gel. We further assessed cell spreading of ECs and MSCs in the z-plane in IMARIS (version 9.9, Abingdon, UK). Briefly, a volume was created from z-stacks taken of the spheroids, and sprout length was measured from the 3D reconstructions.

VEGF and MMP-2 secretion from entrapped EC-MSC spheroids were quantified using cytokine-specific enzyme-linked immunoassay (ELISA) kits according to the manufacturer's protocol (R&D Systems, Minneapolis, MN). The secretory profile of EC-MSC spheroids in the degradable hydrogels was characterized with a ProcartaPlex™ human angiogenesis panel 18-plex kit to measure angiopoietin-1, BMP-9, EMMPRIN, follistatin, HB-EGF, LYVE-1, TIE-2, CD31, EGF, FGF-2, G-CSF, HGF, IL-8, leptin, PDGF-BB, syndecan, VEGF-A, and VEGF-D (CN: EPX180-15806-901; ThermoFisher) and assessed on the Luminex® xMAP 200 (ThermoFisher). The net mean fluorescence intensity (MFI) was measured and calculated for the 7 standards and samples, and the data were analyzed using the online ProcartaPlex™ Analysis Application. GFP+ ECs were co-cultured with MSCs stained with CellTrace™ Far Red (Invitrogen) to discern cellular spreading in the gels. Spheroids were imaged using confocal microscopy (Leica STELLARIS, Leica Camera AG, Wetzlar, Germany).

To interrogate the influence of gel degradation on the proangiogenic potential of EC-MSC spheroids, spheroid-loaded PEG-4MAL gels were treated with 50 μM GM6001 (Sigma-Aldrich) and 0.2 μM Latrunculin A (LatA; Abcam, Cambridge, MA), an inhibitor that blocks the polymerization of actin filaments. We then quantified relative gene expression of *VEGF* and *HGF* by quantitative real-time polymerase chain reaction (qRT-PCR). Samples were collected in 0.5 mL of TRIzol Reagent (Invitrogen) and homogenized. RNA was isolated following instructions per the manufacturer. 800 ng of RNA was reverse transcribed using the QuantiTect Reverse Transcription Kit (Qiagen, Hilden, Germany) and normalized to a final concentration of 10 ng/μL. We performed qRT-PCR using *Taq* PCR Master Mix (Qiagen) in a QuantStudio 6 Pro real-time PCR system (ThermoFisher). Human specific primers *VEGF* (Hs00900055_m1) and *HGF* (Hs00300159_m1) were used (ThermoFisher). Critical threshold values (Ct) were quantified for each gene of interest with a ΔCt value quantified by subtracting the samples Ct value of the *GAPDH* house-keeping gene. The ΔΔCt value was quantified by subtracting the average ΔCt value of the untreated groups (non-RGD modified, LatA treated PEG-DT) from each sample. Expression values for each gene were then represented as $2^{-\Delta\Delta Ct}$.

2.5. Evaluating wound healing via ex vivo skin explant model

We assessed the influence of matrix degradation on wound healing in a full thickness human skin *ex vivo* model. Human discarded skin explants (Genoskin; Toulouse, France) were suspended in 12-well plates using inserts to create an air-liquid interface during culture. We generated partially degradable (GPQ-A:PEG-DT) and non-degradable (PEG-DT) PEG-4MAL gels and encapsulated EC-MSC spheroids at 5×10^6 cells/mL. The cell concentration was scaled to maintain consistency between the number of cells entrapped in the gels for *ex vivo* treatment and the number of cells entrapped in the gels for *in vitro* characterization. Gels were synthesized in 4 mm diameter circular silicone molds and allowed to reach equilibrium by swelling for 24 h before application to the wound. On the day of arrival, we created a burn injury on the skin explant using a soldering iron with a chiseled attachment (4 mm in diameter) by applying the tip to the surface of the skin with a light pressure for 5 s (Video A.1). The distance between the soldering iron and the stand holding the plate was marked and kept constant for each *ex vivo* skin explant to achieve consistent wound size and depth. Burns were subsequently rinsed three times with phosphate buffered saline (PBS) before treating the wound surface with PEG-4MAL gels. Unwounded explants were used as a positive control while wounded, untreated explants were the negative control. PEG-4MAL gels were left undisturbed, and 3:1 media (20 μL) was applied on top of the hydrogel every 2 d to retain the scaffold's moisture. Explants were cultured using culture media (Genoskin) with media changes every 2 d. On day 7, skin explants were fixed in formalin at 4°C overnight and washed with PBS prior to paraffin embedding and sectioning for histology. Photographic images were taken of the wounds immediately after wounding and after 7 d in culture. *Ex vivo* models were collected on day 7 to focus on the inflammatory and early proliferation stages of the wound healing cycle where MMPs are prevalent. This time point enabled us to better characterize the influence of co-culture spheroid-entrapped degradable gels on tissue repair.

Samples were sectioned at 6–8 μm thickness, stained for Masson's trichome staining. and imaged at 4X and 10X using a Nikon TE2000U microscope. The entire epidermal layer of at least 5 slides per group were imaged. To examine the effects of gel degradation on epidermal regeneration, 4 epidermal thickness measurements were taken from 3 representative images per group. Measurements were taken from the deepest portion of the dermis (*stratum basale*) to the end of the *stratum spinosum*. For immunohistochemical staining, samples were rehydrated followed by heat-mediated antigen retrieval with sodium citrate buffer and incubation in blocking buffer for 1 h at room temperature. Slides were incubated with anti-collagen 1 (1:100 dilution, ab34710; Abcam) and anti-cytokeratin 14 (1:200 dilution, ab7800; Abcam) antibodies at 4°C overnight. Slides were then treated with goat anti-mouse antibody conjugated to Alexa Fluor 568 (1:500; ab175473; Abcam) and goat anti-rabbit antibody conjugated to Alexa Fluor 647 (1:500; ab150083; Abcam). Slides were also incubated with DAPI (ThermoFisher) as a counterstain. Characteristics of the epidermis, dermis, and wound area were observed from 3 fields of view on at least 3 different slides per group using a confocal microscope (Leica STELLARIS).

2.6. Statistical analysis

Data are derived from a minimum of three independent experiments, where each are comprised of at least three gels, and presented as means ± standard deviation. Statistical significance was assessed by one-way ANOVA with Tukey's multiple comparisons test or Student's t-test when appropriate. *P*-values ≤ 0.05 were considered statistically significant. Statistical analysis was performed using GraphPad Prism® 9 software (GraphPad Software, San Diego, CA). Significance is denoted by alphabetical letterings or asterisks or hashtags. Different letters denote statistical significance between groups, while data sharing a letter are not statistically different from one another. * or # ($p \leq 0.05$),

** or ## ($p \leq 0.01$), *** or ### ($p \leq 0.001$). # indicates significance between that group and corresponding GPQ-A groups.

3. Results

3.1. Characterization of PEG-4MAL hydrogel degradation

PEG-4MAL hydrogels were formulated with varying percentages of MMP-degradable (*i.e.*, GPQ-A) and non-degradable (*i.e.*, PEG-DT) crosslinkers to develop three groups with varying degradation capacities – fully degradable (GPQ-A), partially degradable (GPQ-A:PEG-DT), and non-degradable (PEG-DT) (Fig. 1A). Following gel synthesis, acellular PEG-4MAL hydrogels measured 8 mm in diameter. After achieving maximum swelling in media for 24 h, gels swelled to 13 mm in diameter for all groups (Fig. 1B). All hydrogels exhibited similar initial storage moduli. By day 7, we observed decreases in storage moduli in gels containing GPQ-A. Fully degradable gels exhibited an 80% decrease in storage modulus on day 7 (133 ± 46 Pa, $p = 0.002$) compared to day 1 (673 ± 117 Pa) (Fig. 1C). Partially degradable gels demonstrated a downward trend in storage modulus on day 7 (378 ± 67 Pa, $p = 0.105$) compared to day 1 (784 ± 331 Pa), although not significant. Non-degradable gels exhibited no differences, indicating there was no gel degradation over 7 days.

The wet and dry mass were measured to further assess gel degradation. We did not detect differences in wet or dry mass on day 7 for the different gel formulations (Fig. 1D and E). The differences in storage moduli after one week for the various degradable gels, despite the absence of cells, could be attributed to the presence of MMPs in the fully supplemented media [37], hydrogel swelling, or increased mesh density. Collectively, these data demonstrate the tunable nature of PEG-4MAL gels achievable by varying GPQ-A concentration.

3.2. GPQ-A concentration mediates gel degradation by EC-MSC spheroids

EC-MSC spheroids were encapsulated in PEG-4MAL hydrogels with varying amounts of GPQ-A to investigate the influence of cells on gel mechanical properties and degradation. Gels crosslinked with GPQ-A exhibited significant decreases in storage moduli. Fully degradable gels had a 64% decrease from day 1 (579 ± 137 Pa) to day 7 (207 ± 81 Pa, $p = 0.006$) and partially degradable gels had a 50% decrease from day 1 (800 ± 255 Pa) to day 7 (400 ± 107 Pa, $p = 0.012$) (Fig. 2A). This could be attributed to potential MMPs in the culture medium serum

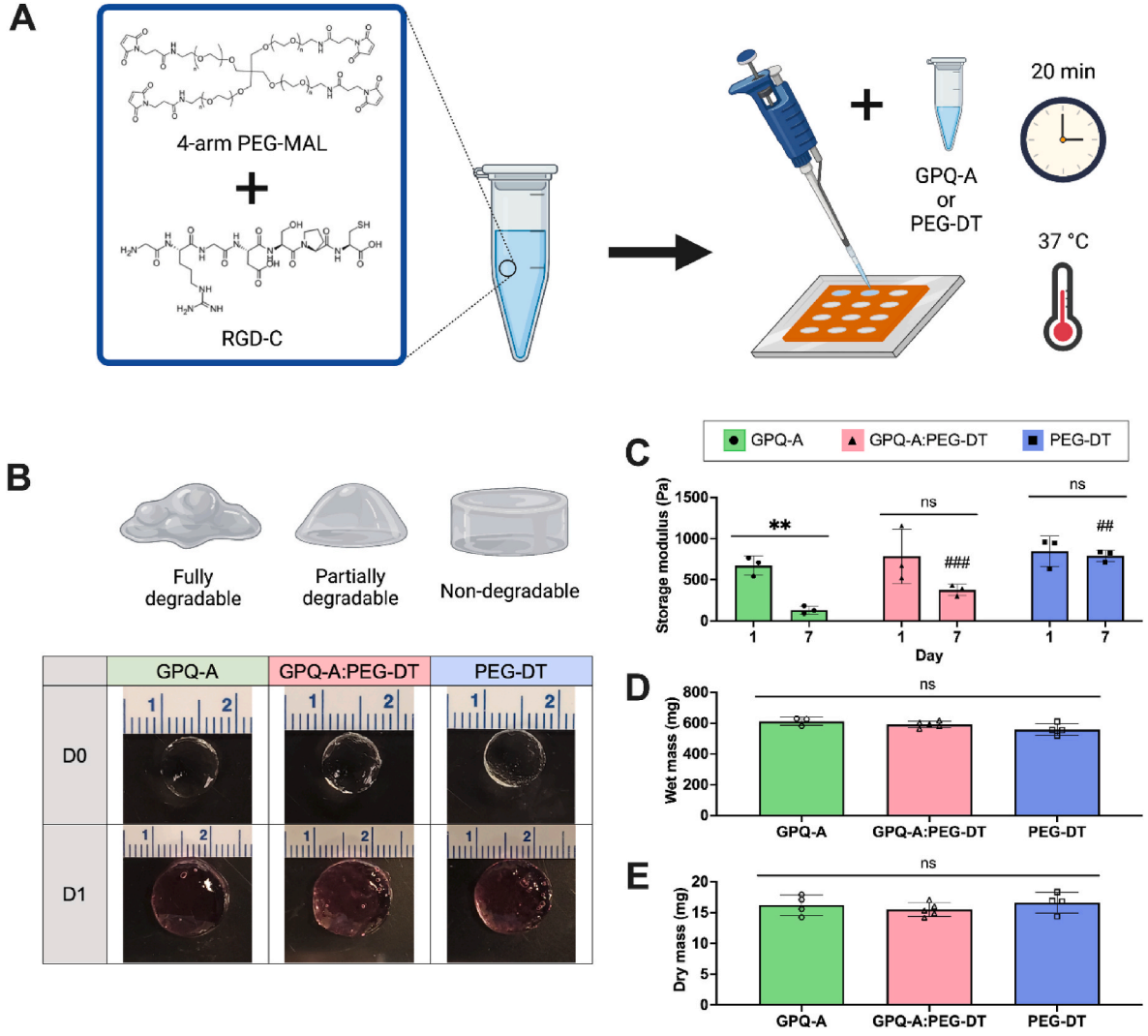

Fig. 1. PEG-4MAL hydrogel degradation is modulated by varying GPQ-A concentration. (A) Schematic of PEG-4MAL hydrogel synthesis with protease degradable (GPQ-A) and non-degradable (PEG-DT) crosslinkers. **(B)** Gross morphological images of fully degradable (GPQ-A), partially degradable (GPQ-A:PEG-DT), and non-degradable (PEG-DT) hydrogels upon synthesis and post-24 h swelling. **(C)** Storage modulus of PEG-4MAL gels over 7 days ($n = 3$). **(D)** Wet and **(E)** dry mass remained similar for various gel formulations on day 7 ($n = 3$–5). Significance is denoted by asterisks or hashtags where ** or ## ($p \leq 0.01$), *** or ### ($p \leq 0.001$). # indicates significance between that group and corresponding GPQ-A groups.

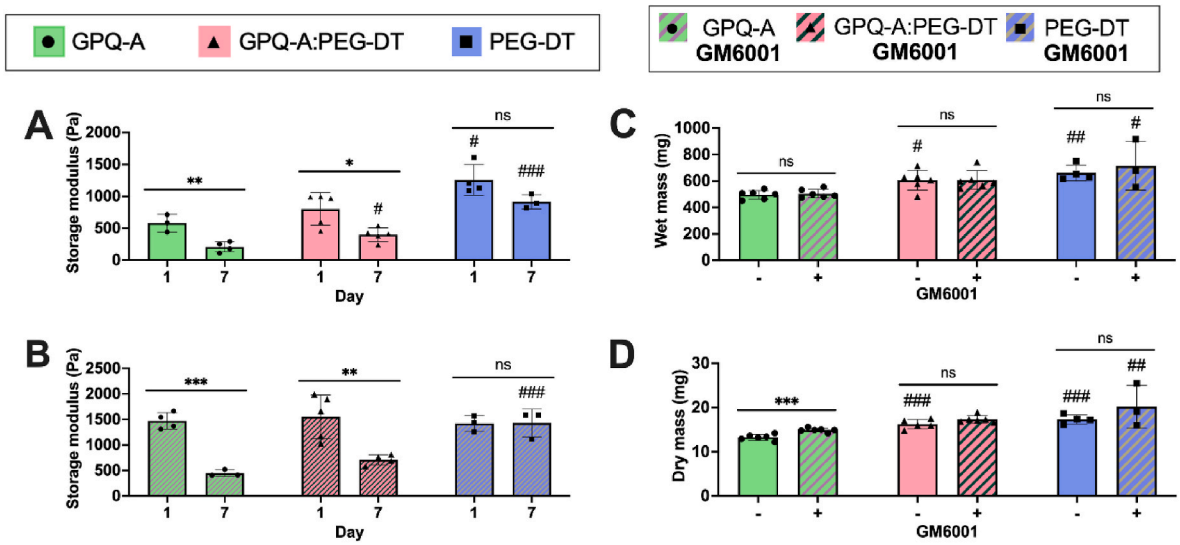

Fig. 2. PEG-4MAL hydrogel degradation by EC-MSC spheroids is dependent on GPQ-A. (A) Storage modulus of spheroid-loaded PEG-4MAL gels over 7 days (n = 3–5). **(B)** Storage modulus of spheroid-loaded PEG-4MAL gels treated with GM6001 over 7 days (n = 3–5). **(C)** Wet and **(D)** dry mass of EC-MSC spheroid encapsulated gels on day 7 with or without GM6001 (n = 3–6). Significance is denoted by asterisks or hashtags where * or # ($p \leq 0.05$), ** or ## ($p \leq 0.01$), *** or ### ($p \leq 0.001$). # indicates significance between that group and corresponding GPQ-A groups.

[37]. Non-degradable gels had a slight but non-significant decrease in storage modulus from day 1 (1141 ± 60 Pa) to day 7 (914 ± 110 Pa, p = 0.071). As GPQ-A concentration increased, gels exhibited greater degradation on day 1, characterized by decreased storage moduli. These differences were more prominent on day 7. Gel degradation was further analyzed by measuring wet and dry mass of spheroid-loaded gels. On day 7, the wet mass was inversely related to GPQ-A concentration (Fig. 2C). This trend was also observed with the dry mass. Partially degradable gels (16.2 ± 1.1 mg, $p \leq 0.001$) weighed 1.2 times more than fully degradable gels (13.3 ± 0.7 mg) and non-degradable gels (17.3 ± 1.0 mg, $p \leq 0.001$) weighed 1.3 times more than fully degradable gels (Fig. 2D). Overall, in the presence of EC-MSC spheroids, PEG gels with higher GPQ-A concentration exhibited greater degradation evidenced by the inverse relationship between GPQ-A and storage moduli and wet/-dry mass.

To evaluate if the cleavage of MMP-susceptible sites was responsible for gel degradation, we cultured the spheroid-entrapped hydrogels in GM6001-treated media to limit MMP activity. On day 1, GPQ-A crosslinked gels treated with GM6001 (GPQ-A, 1471 ± 162 Pa, p = 0.977; GPQ-A:PEG-DT, 1548 ± 429 Pa, p = 0.846) had storage moduli similar to those of non-degradable gels treated (1423 ± 157 Pa) (Fig. 2B). Upon GM6001 treatment, the storage moduli for GPQ-A and GPQ-A:PEG-DT remained ~110% higher than their non-treated counterparts, suggesting that differences in storage moduli are due to hydrogel degradation by the entrapped spheroids. To further determine if gel degradation was cell-mediated, we compared the mechanical properties of acellular gels on day 1 with and without GM6001-treated media (Fig. A1). There were no significant differences in storage moduli, suggesting that the decrease in storage moduli observed in cellular loaded gels treated with GM6001 (Fig. 2B) was due to cell-mediated degradation. Degradation was also observed in the wet and dry mass of the GM6001-treated PEG gels on day 7 (Fig. 2C and D). Some degradation was present, evidenced by the lower dry mass of GPQ-A (14.9 ± 0.4 mg) gels compared to GPQ-A:PEG-DT (17.3 ± 0.8 mg, p = 0.145) and PEG-DT (20.2 ± 4.8 mg, p = 0.009) groups. However, GM6001 reduced matrix degradation as demonstrated by the ~1.1-fold increase in dry mass of GM6001-treated versus non-treated gels. The differences in dry mass observed between GM6001-treated and non-treated GPQ-A gels, coupled with the small differences in wet mass between these groups, suggest that gel degradation occurred but not at a level that compromised the integrity of the gel.

These data establish that the degree of hydrogel degradation by EC-MSC spheroids is dependent on the concentration of GPQ-A crosslinker. Furthermore, the inhibition of MMP-degradation *via* GM6001 validates that matrix degradation is due to enzymatic cleavage of MMP-susceptible sites in the gel and is in agreement with prior reports [38].

3.3. EC-MSC spheroid proliferation and metabolic activity is dependent on gel degradation

We then investigated the influence of gel degradation on EC-MSC spheroid function by controlling the concentration of GPQ-A crosslinker. Incorporated EC-MSC spheroids were 442 ± 24 μm in diameter (n = 3). MMPs, specifically MMP-2, are associated with extracellular matrix degradation throughout the body and especially in the skin. On day 1, MMP-2 secretion from EC-MSC spheroids was comparable for all groups but by day 7, we detected greater MMP-2 secretion by cells entrapped in gels more vulnerable to degradation (*i.e.*, gels with higher GPQ-A concentration) (Fig. 3A).

EC-MSC spheroids in GPQ-A gels (3.1 ± 0.3 ng MMP-2/ng DNA) had 1.8-fold and 3.7-fold more MMP-2 secretion compared to GPQ-A:PEG-DT (1.77 ± 0.44 ng MMP-2/ng DNA, $p \leq 0.001$) and PEG-DT (0.85 ± 0.17 ng MMP-2/ng DNA, $p \leq 0.001$), respectively. Over 7 days, spheroids in all groups remained viable (Fig. 3B). All gel formulations supported proliferation, which was marked by an increase in total DNA content from day 1 to day 7 (Fig. 3C). We did not detect differences among groups on days 1 or 7. This demonstrates that PEG-4MAL gels promoted cell proliferation and suggests that gel degradation did not impact the proliferative capabilities of the cells. Interestingly, metabolic activity of the cells increased for degradable groups yet decreased for the non-degradable group. Metabolic activity of cells in fully degradable gels increased 135% from day 1 (15.3 ± 7.7 RFU/ng DNA) to day 7 (36.0 ± 4.5 RFU/ng DNA, p = 0.004) while the activity in partially degradable gels increased 69% from day 1 (8.9 ± 3.8 RFU/ng DNA) to day 7 (15.0 ± 3.8 RFU/ng DNA, p = 0.047). However, metabolic activity of spheroids in non-degradable gels decreased 65% from day 1 (18.8 ± 7.6 RFU/ng DNA) to day 7 (6.7 ± 1.4 RFU/ng DNA, p = 0.02) (Fig. 3D). On day 7, we observed distinct differences in metabolic activity among the GPQ-A, GPQ-A:PEG-DT, and PEG-DT gels. There was a positive correlation between metabolic activity and GPQ-A concentration. These data indicate that the degree of gel degradation has no effect on the proliferative

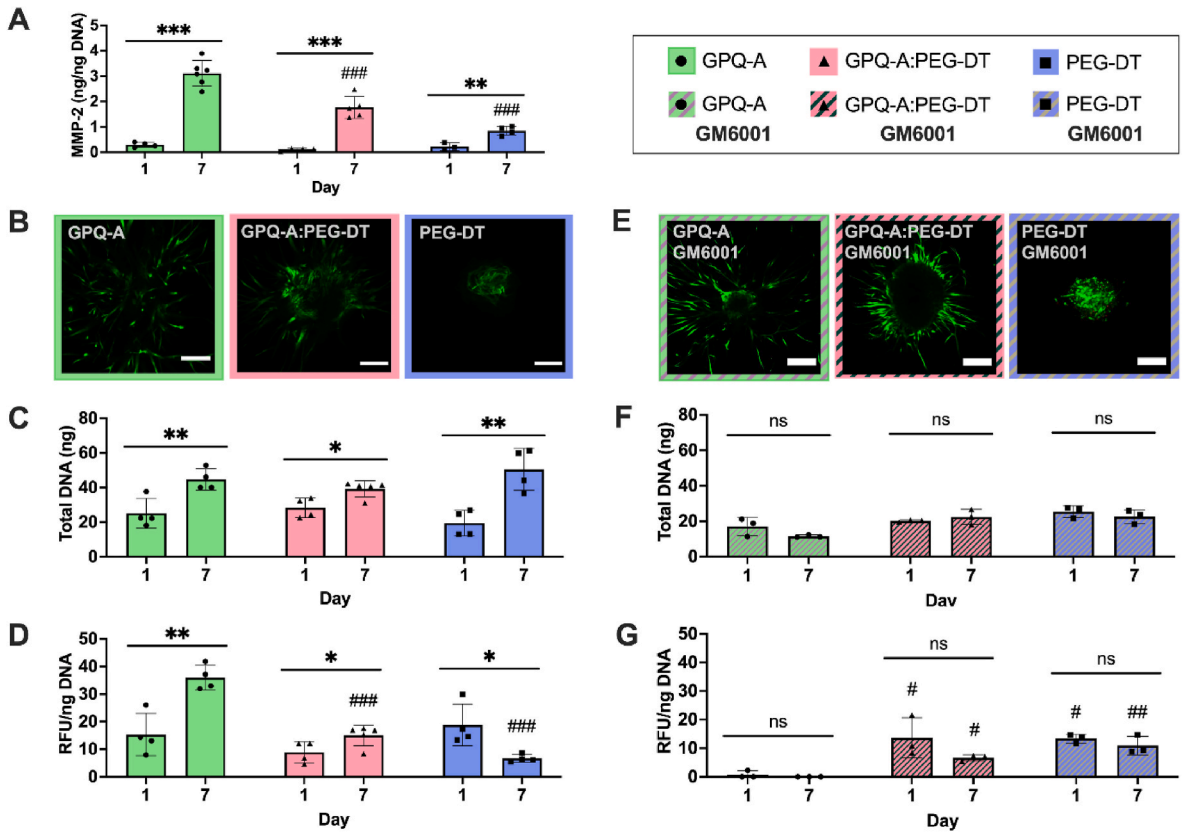

Fig. 3. PEG-4MAL hydrogel degradation regulates EC-MSC spheroid proliferation and metabolic activity. (A) Normalized MMP-2 secretion from EC-MSC spheroids is higher in more degradable gels over 7 days (n = 3–6). **(B)** Live/Dead stain demonstrates ECs and MSCs remained viable after 7 days in all gels. Scale bars are 200 μm. **(C)** Total DNA and **(D)** metabolic activity of spheroids in PEG gels over 7 days (n = 4–5). **(E)** Live/Dead staining confirms ECs and MSCs remained viable after 7 days in gels with GM6001 treatment. Scale bars are 200 μm. **(F)** Total DNA content and **(G)** metabolic activity of GM6001-treated spheroids in PEG gels was impaired over 7 days (n = 3). Significance is denoted by asterisks or hashtags where * or # ($p \leq 0.05$), ** or ## ($p \leq 0.01$), *** or ### ($p \leq 0.001$). # indicates significance between that group and corresponding GPQ-A groups.

capacity of EC-MSC spheroids, but gel degradation influences the metabolic activity of entrapped cells.

When treated with GM6001, proliferation was inhibited in all groups with total DNA mass ranging between 17 and 25 ng over 7 days (Fig. 3F). However, despite the consistent DNA content, metabolic activity varied strikingly for the different degradable gels (Fig. 3G). GM6001 markedly suppressed metabolic activity in fully degradable gels on days 1 and 7. To ensure the cells were not negatively affected by GM6001 treatment, we evaluated cell viability *via* Live/Dead and found the cells remained viable with MMP-inhibitor treatment (Fig. 3E). Treatment with GM6001 inhibited both proliferation and metabolic activity in the degradable gels. To investigate if the inhibition of cellular proliferation was due to GM6001 treatment itself or restriction of gel degradation, we treated EC-MSC spheroids with GM6001 immediately after spheroid formation while in the agarose molds (Fig. A2). Treatment with GM6001 exhibited no effect on cell proliferation on day 7, suggesting that hydrogel degradation is critical for cellular proliferation. However, metabolic activity of cells in the fully degradable gels was negatively impacted, evidenced by the minimal to no activity on days 1 and 7. This behavior could be attributed to the gels being allowed to reach swelling equilibrium in culture media for 24 h prior to GM6001 treatment. These findings emphasize the significant role that matrix degradation has on the bioactivity of EC-MSC spheroids.

3.4. Cellular outgrowth from EC-MSC spheroids is mediated by hydrogel degradation

Matrix remodeling is critical in the wound healing cascade to enable the migration of cells within the wound bed. We assessed cell spreading of ECs and MSCs in two dimensions (2D) from the spheroids in degradable gels by quantifying the number of protrusions and the protrusion lengths in individual z-planes (Fig. 4A).

On day 1, we observed more than 2-fold more protrusions for spheroids in fully degradable gels (6.8 ± 3.5 protrusions) than spheroids in partially (3.1 ± 1.8 protrusions, $p = 0.041$) and non-degradable (2.4 ± 1.3 protrusions, $p = 0.037$) gels (Fig. 4B). Average sprout length for these groups exhibited a similar trend where spheroids in fully degradable gels (125 ± 14 μm) had 1.2-fold longer protrusion lengths than the other groups (GPQ-A:PEG-DT, 103 ± 12 μm, $p = 0.013$; PEG-DT, 107 ± 5 μm, $p = 0.032$) (Fig. 4C). By day 7, degradable gels enabled a plethora of cellular outgrowth, while we observed few protrusions in non-degradable gels (2.7 ± 1.6 protrusions, $p \leq 0.001$). Interestingly, average sprout length increased for fully (393 ± 59 μm, $p \leq 0.001$) and partially (220 ± 30 μm, $p = 0.001$) degradable gels while the outgrowth of cells was stunted in non-degradable gels (109 ± 7 μm). Outgrowth length was dependent on GPQ-A concentration. The sprout length in GPQ-A gels increased 3.1-fold from day 1 to day 7 (393 ± 59 μm, $p = 0.046$) while GPQ-A:PEG-DT gels increased 2.1-fold from day 1 to day 7 (220 ± 30 μm, $p \leq 0.001$). We further assessed cellular protrusions in three-dimensional (3D) culture and observed longer sprout lengths for spheroids in degradable gels (GPQ-A, 961 ± 132 μm, $p \leq 0.001$; GPQ-A:PEG-DT, 789 ± 55 μm, $p \leq 0.001$) compared to non-degradable gels (0 μm) (Fig. 4D and E). There were no differences in sprout lengths between spheroids in fully and partially degradable gels. These data demonstrate that a microenvironment that facilitates matrix remodeling enables more cellular protrusions and longer outgrowths

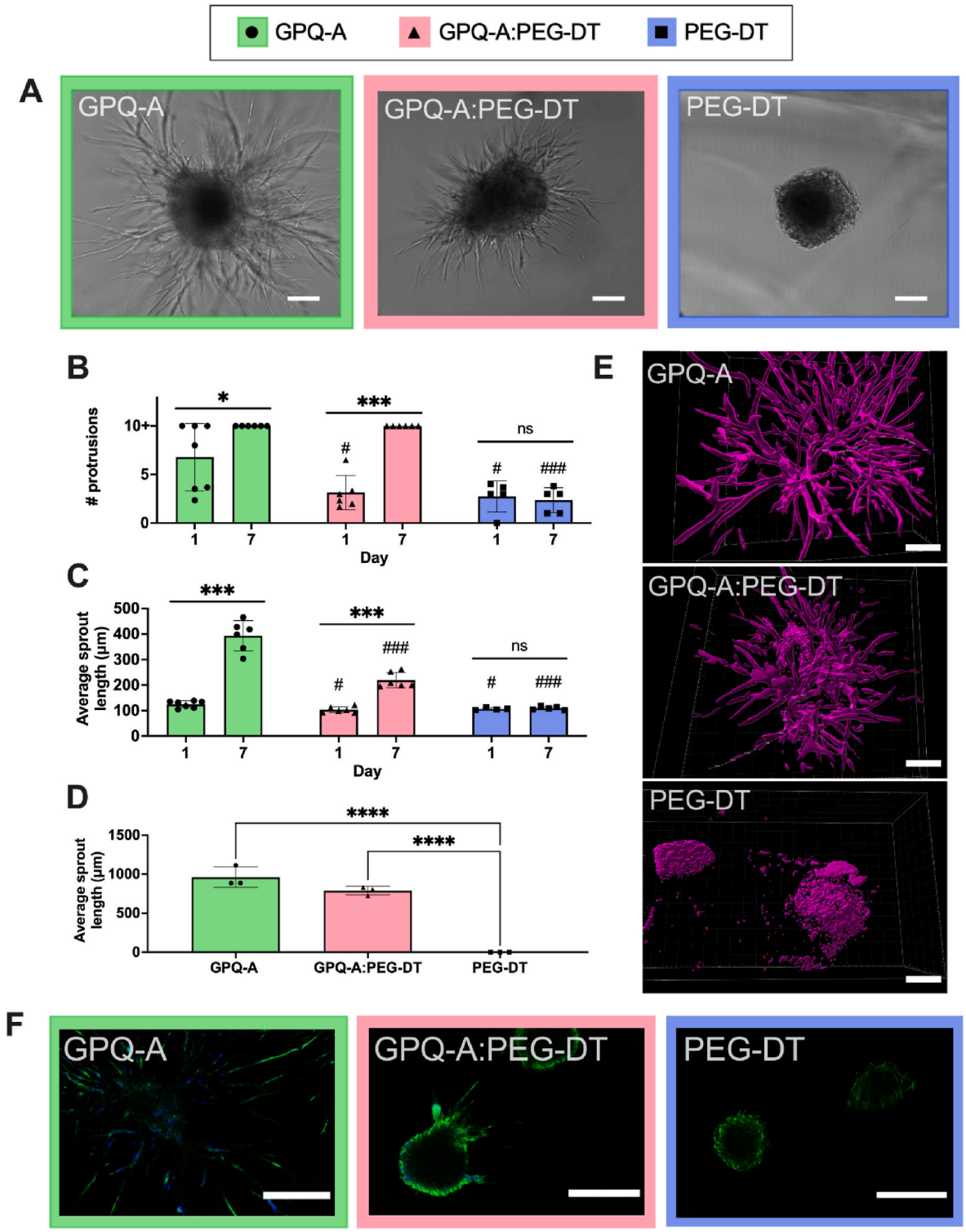

Fig. 4. Degradable PEG-4MAL hydrogels regulate cellular outgrowth from EC-MSC spheroids. (A) Spheroid morphology on day 7 reveals degrees of spheroid spreading. Scale bars are 200 μm. **(B)** Number and **(C)** average sprout length of EC and MSC protrusions of spheroids in degradable gels positively correlated with GPQ-A concentration ($n = 5$–7). **(D)** Quantification of average sprout length of EC and MSC protrusions in 3D for GPQ-A crosslinked groups and visualized in **(E)** rendered 3D volumes of spheroids in gels on day 7. Scale bars are 200 μm. **(F)** Spheroids stained with phalloidin (green) for actin and DAPI (blue) for cell nuclei on day 7 ($n = 4$–7). Scale bars are 500 μm. Significance is denoted by asterisks or hashtags where * or # ($p \leq 0.05$), *** or ### ($p \leq 0.001$), **** ($p \leq 0.0001$). # indicates significance between that group and corresponding GPQ-A groups. (For interpretation of the references to color in this figure legend, the reader is referred to the Web version of this article.)

compared to non-degradable gels, emphasizing the importance of matrix remodeling on cellular migration of EC-MSC spheroids.

The effect of gel degradation on cellular morphology was further investigated using actin filament (F-actin) staining after culturing spheroids for 7 days (Fig. 4F). Most of the cells within GPQ-A hydrogels exhibited significant elongation and spreading from the spheroid core. In GPQ-A:PEG-DT gels, we observed some elongated cells from the spheroid, demonstrated by the slightly spread, aligned, thick filaments throughout and along the periphery of the spheroid. In contrast, cells in non-degradable PEG-DT gels were slightly elongated within the spheroid but remained in spheroidal form, evidenced by the lack of cell spreading at the spheroid edge, emphasizing the importance of hydrogel degradation on F-actin structure and orientation. Cells along the edge of the spheroids were oriented slightly parallel to the edge. Overall, gels with higher degradability promoted more elongated protrusions oriented outwardly from the spheroid core.

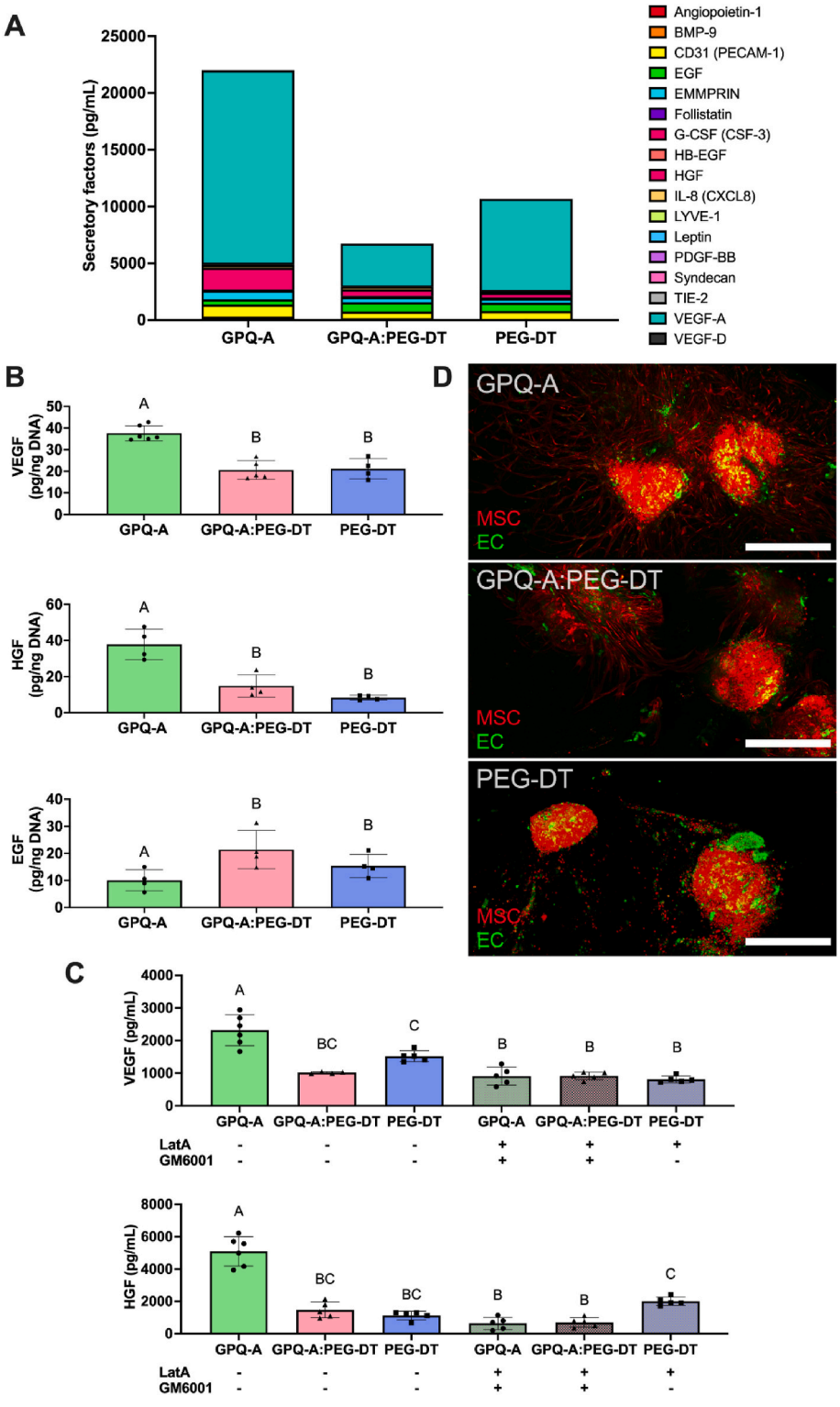

Fig. 5. Fully degradable PEG-4MAL hydrogels enhance the proangiogenic potential of EC-MSC spheroids and modulate EC outgrowth. (A) Angiogenic cytokine content in the secretome of EC-MSC spheroids in degradable hydrogels on day 7. **(B)** Normalized VEGF, HGF, and EGF secretion from EC-MSC spheroids is modulated by gel degradation on day 7 ($n = 4–6$). **(C)** Total VEGF and HGF secretion from EC-MSC spheroids treated with 0.2 μM LatA and 50 μM GM6001 on day 7 ($n = 4–6$). **(D)** Fluorescently stained ECs (green) and MSCs (red) after 7 days showcase degradable gels supported EC outgrowth. Scale bars are 500 μm. Significance is denoted by alphabetical lettering where different letters denote statistical significance between groups. (For interpretation of the references to color in this figure legend, the reader is referred to the Web version of this article.)

3.5. Gel degradation enhances proangiogenic potential of EC-MSC spheroids and modulates EC outgrowth

Chronic wounds are marked by impaired angiogenesis. In light of data emphasizing the influence of hydrogel degradation on metabolic activity and sprouting of entrapped cells, we characterized the angiogenic secretory profiles of spheroids in gels with varying degradability. Of the analytes examined, spheroids in fully degradable formulations secreted 22,018 pg/mL angiogenic cytokines while cells in partially degradable gels secreted 6,729 pg/mL and cells in non-degradable gels secreted 10,671 pg/mL (Fig. 5A). The secretome of spheroids from GPQ-A groups was primarily composed of VEGF-A (77%), with HGF (8.6%), CD31 (4.7%), EMMPRIN (3.5%), EGF (2.1%), IL-8 (1.1%) and trace amounts of the other analytes. For GPQ-A:PEG-DT, the secretome was also primarily composed of VEGF-A (55%), with EGF (12%), HGF (8.7%), CD31 (9.1%), EMMPRIN (7%), IL-8 (3.6%) and trace amounts of the other analytes. Spheroids in PEG-DT exhibited a secretome composition similar to GPQ-A: VEGF-A (75%), EGF (7%), CD31 (6.5%), HGF (3.8%), EMMPRIN (3.5%), and IL-8 (1.7%). Despite relatively comparable secretome composition, fully degradable gels (37.5 ± 3.5 pg VEGF/ng DNA) promoted ~1.8-fold more VEGF secretion from EC-MSC spheroids compared to partially (20.6 ± 4.3 pg VEGF/ng DNA, $p \leq 0.001$) and non-degradable (21.1 ± 4.7 pg VEGF/ng DNA, $p \leq 0.001$) gels after 7 days (Fig. 5B). Spheroids in fully degradable gels (37.9 ± 8.5 pg HGF/ng DNA) also secreted HGF levels 2.5-fold and 4.6-fold higher than partially (14.9 ± 6.1 pg HGF/ng DNA, $p \leq 0.01$) and non-degradable (8.3 ± 1.3 pg HGF/ng DNA, $p \leq 0.001$) gels, respectively. Interestingly, spheroids in partially degradable hydrogels (21.4 ± 7.0 pg EGF/ng DNA) exhibited the highest levels of EGF compared to fully degradable (10.0 ± 3.9 pg EGF/ng DNA, $p = 0.033$) and non-degradable (15.4 ± 4.3 pg EGF/ng DNA, $p = 0.289$) hydrogels. These data emphasize that matrix degradation promotes distinct yet complex secretory profiles and enhances proangiogenic trophic factor secretion with increasing degradation.

Given the influence of degradation on EC-MSC spheroid secretome and cellular spreading (Fig. 4D and E), we investigated the interplay of cell migration, which increases with matrix degradability, and proangiogenic potential of spheroids. Migration was inhibited by treating spheroids entrapped in PEG gels with 0.1 μM latrunculin A (LatA), an inhibitor that blocks actin filament polymerization. However, LatA alone was insufficient to inhibit migration. We observed elongated cellular protrusions and a ring of cells surrounding the spheroid core by day 7 in degradable hydrogels (Fig. A3), potentially due to scaffold degradation. Therefore, we treated the spheroids with various combinations of GM6001 and LatA to control for confounding effects from matrix degradation and found cellular migration was sufficiently inhibited when treated with 0.2 μM LatA and 50 μM GM6001 (Fig. A4).

Moving forward with these concentrations, we hypothesized that treatment with LatA and GM6001 would promote similar expression of angiogenesis-related genes (*i.e.*, *VEGF* and *HGF*) in spheroids in degradable gels compared to those in non-degradable gels. We also treated PEG-DT groups with LatA to account for actin polymerization as a confounding factor. Non-RGD modified groups treated with GM6001 served as a negative control. On day 7, we did not detect significant differences in *VEGF* expression by spheroids in degradable and non-degradable hydrogels, emphasizing hydrogel degradation is necessary for increased *VEGF* expression (Fig. A5). Interestingly, compared to treated non-RGD modified groups, there was slightly higher *VEGF* expression across all treated RGD-modified groups. This suggests that the proangiogenic potential of spheroids is influenced by both migration and gel degradation, as well as cellular adhesion. We also quantified *HGF* expression, which plays multiple roles during wound healing by promoting proliferation, migration, and angiogenesis in epithelial cells as well as dedifferentiation of epidermal cells [39]. Due to the significant degradation exhibited by GPQ-A gels by day 7 and with an eye toward translation to the wounded *ex vivo* skin model, we focused on partially (GPQ-A:PEG-DT) and non-degradable (PEG-DT) groups. Like *VEGF* expression, *HGF* expression in spheroids was comparable between the partially and non-degradable scaffolds. *HGF* expression for non-RGD modified groups was also slightly lower than RGD-modified ones, further emphasizing the potential contributing role of cell adhesion on gene expression.

We further evaluated the influence of LatA and GM6001 on VEGF and HGF secretion and observed significant reduction in secretion levels in the degradable groups when treated with both inhibitors (Fig. 5C). Inhibition of VEGF secretion by EC-MSC spheroids was more prominent in the GPQ-A group on day 7, evidenced by the nearly 50% reduction in VEGF secretion in LatA and GM6001 treated versus cells in non-treated gels. The total VEGF secreted in GPQ-A and GPQ-A:PEG-DT gels were similar to those in PEG-DT gels suggesting that degradation is imperative for proangiogenic cytokine secretion. This was corroborated by similar trends in HGF secretion. LatA and GM6001 substantially reduced HGF secretion in GPQ-A and GPQ-A:PEG-DT scaffolds compared to non-treated counterparts. Interestingly, cells in PEG-DT treated groups exhibited more than twice the total HGF secretion of cells in degradable constructs, albeit not significantly different from non-treated PEG-DT. Together, these data suggest that migration, which is promoted by more degradable matrices, facilitates the secretion of proangiogenic cytokines.

In conjunction with quantifying proangiogenic factors, spheroids composed of GFP+ ECs and CellTraced MSCs were imaged after 7 days in these gels to visualize cell specific outgrowth (Fig. 5D). Fully or partially degradable gels facilitated outward spreading of MSCs. MSCs exhibited elongated, spindle-shaped morphology which protruded and extended from the spheroid cores. In the vicinity of other spheroids, MSCs formed aligned cellular structures in the direction of neighboring spheroids. Degradable gels also facilitated some EC migration. On the other hand, non-degradable gels prevented both EC and MSC elongation and spreading.

Altogether, these data emphasize matrix degradation is critical for the production and expression of angiogenesis associated cytokines and genes (*i.e.*, *VEGF* and *HGF*). This synergistic relationship subsequently modulates EC and MSC cellular morphology, migration, and network formation.

3.6. Degradable gels enhanced wound healing in an ex vivo skin model

Matrix degradation is critical for wound healing, and high protease activity from MMPs can lead to chronic nonhealing wounds. We tested the efficacy of EC-MSC spheroid-loaded degradable gels as a potential treatment for burn wounds in an *ex vivo* skin model (Fig. 6A and B). We observed recovery of the stratified architecture of the epidermal layer with both degradable and non-degradable gels (Fig. 6C). Furthermore, wounds treated with non-degradable (PEG-DT) gels exhibited a higher degree of epidermal detachment compared to wounds treated with partially degradable (GPQ-A:PEG-DT) gels. However, there were no discernible differences in wound diameter for groups treated with degradable or non-degradable gels.

Immunofluorescence images revealed more expression of CK14 on the wounds treated with partially degradable gels, suggesting the presence of active basal keratinocytes at the basement membrane (Fig. 6D). This higher CK14 expression supports our findings of better epidermal attachment and accelerated remodeling for wounds treated with partially degradable gels. Furthermore, IHC images revealed no changes in COL1 expression for groups treated with either partially degradable or non-degradable gels compared to the non-treated group at day 7 (Fig. 6D). To further assess epidermal regeneration at day 7, we measured the thickness of the first two epidermal layers *stratum basale* and *stratum granulosum*, characterized by the presence of highly proliferative keratinocytes (Fig. 6E). We detected an increase in epidermal thickness for the *ex vivo* models treated with partially degradable gels (51.27 ± 12.1 μm) compared to non-degradable gels (25.9 ± 4.9 μm)

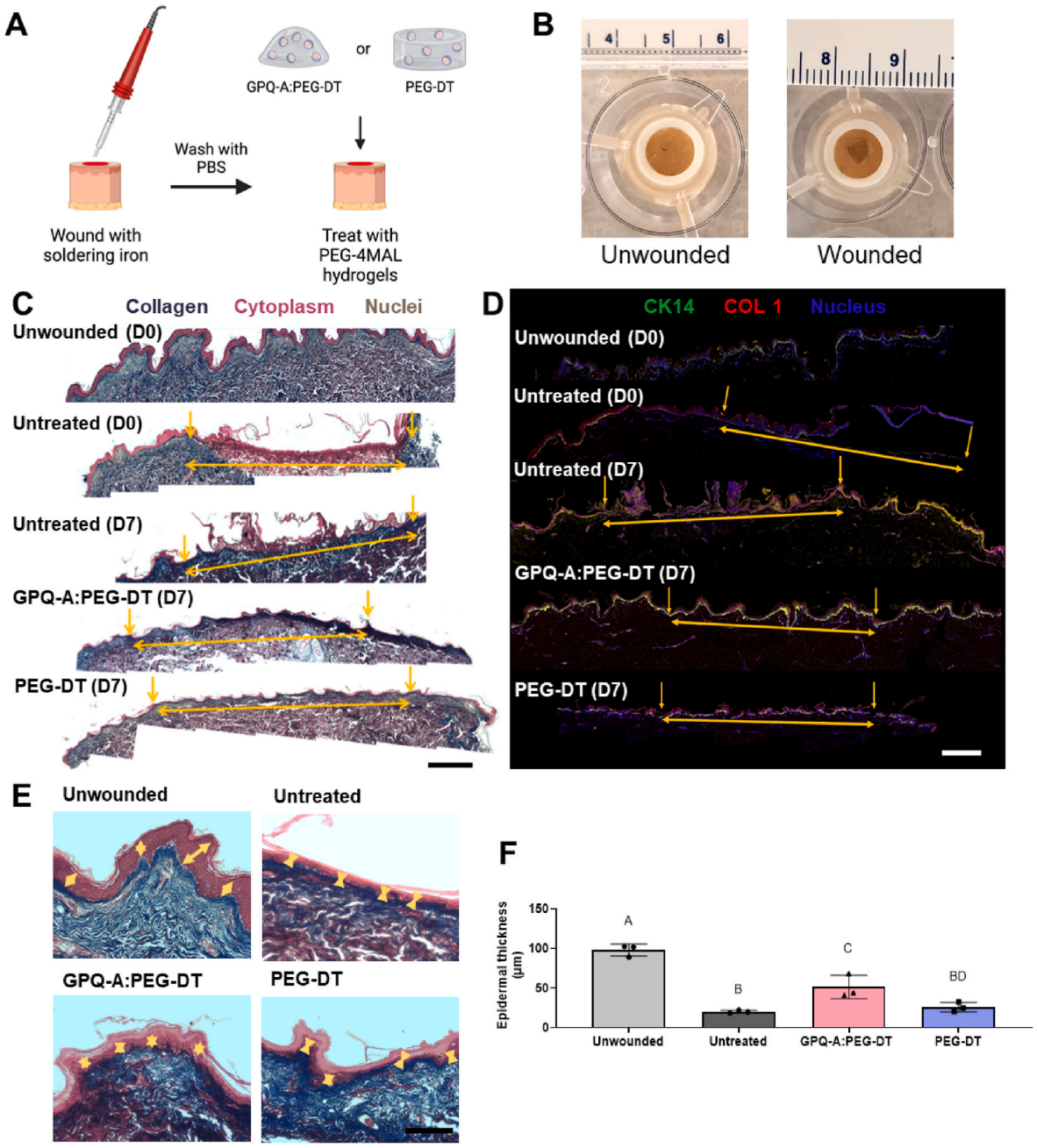

Fig. 6. Partially degradable PEG-4MAL hydrogels with EC-MSC spheroids aid epidermal regeneration and enhance collagen deposition in an *ex vivo* skin model. (A) Schematic of burn procedure in *ex vivo* skin model. **(B)** Skin before and after burn injury. **(C)** Masson's trichrome staining collagen (blue), cytoplasm (pink), and nuclei (brown) reveals collagen deposition and remodeling. Yellow arrows denote the wound area. Scale bar is 1 mm. **(D)** Epidermal regeneration was assessed by immunofluorescent detection of CK14 (green), COL1 (red) and cell nuclei (blue). Scale bar is 1 mm. **(E)** Epidermal thickness was measured on D7 to evaluate the regenerative capabilities of the PEG-4MAL hydrogels. Yellow arrows denote the *stratums basale* and *spinosum*. Scalebar is 100 μm. **(F)** Quantification of epidermal thickness demonstrated improved re-epithelialization for the GPQ-A:PEG-DT treated group on D7. *Groups:* Unwounded (D0) – unwounded skin model control group at day 0; Untreated (D0) – wounded, untreated skin model after burn injury at day 0; Untreated (D7) – wounded, untreated skin model at day 7; GPQ-A:PEG-DT (D7) – wounded skin model treated with a partially degradable (GPQ-A:PEG-DT) hydrogel at day 7; PEG-DT (D7) – wounded skin model treated with a non-degradable (PEG-DT) hydrogel at day 7. (For interpretation of the references to color in this figure legend, the reader is referred to the Web version of this article.)

(Fig. 6F). Moreover, the partially degradable group showed a 52% recovery of the epidermal layer compared to our unwounded control (97.9 ± 6.1 μm), which is significantly higher than the 26% achieved by the non-degradable gel or the 21% of the non-treated group. Collectively, our findings suggest that partially degradable gels improved re-epithelialization and reduction of the wound site at day 7 compared to non-degradable gels.

4. Discussion

Key proteolytic enzymes, such as MMPs, are involved in all stages of the wound healing cascade from regulating inflammation to facilitating the migration of pertinent cells (*i.e.*, vascular ECs, fibroblasts, keratinocytes) *via* ECM degradation [40]. Chronic wounds are marked by high levels of MMPs, which digest growth factors, cell surface receptors and ECM molecules, and consequently delay wound closure [41,42]. Matrix degradation regulates inflammation and the MSC secretome,

establishing its potential as a key modulator of wound healing [43]. However, the influence of matrix degradation on the therapeutic potential of EC-MSC spheroids for wound healing is not well understood. In this study, we used a tunable PEG-based hydrogel to modulate matrix degradation *via* an MMP-cleavable peptide. Using this established platform [27,33], we investigated the influence of matrix remodeling on EC-MSC spheroid function and translated it into a clinically relevant *ex vivo* human skin burn model to evaluate wound healing efficacy.

Natural and synthetic polymers can be formulated to be degradable *via* hydrolytic, oxidative, photolytic, and enzymatic means [44–46]. While natural polymers (*e.g.*, alginate, hyaluronic acid, fibrin) are biocompatible, they often facilitate limited control over tunable degradation [47]. Synthetic polymers, like PEG, offer a blank slate to design a material with specific mechanical properties and degradable moieties [29,48]. Here, we demonstrated the ease of modulating hydrogel degradation by varying GPQ-A concentration in PEG-4MAL gels, similar to prior studies [27]. PEG-4MAL is highly hydrophilic, evidenced by substantial swelling after 24 h in media. The type of crosslinker (*i.e.*, GPQ-A or PEG-DT) had no effect on the degree of swelling. In acellular hydrogels, the storage moduli were around 750 Pa for all groups on day 1. By day 7, there was a decrease in storage moduli as GPQ-A concentration was increased despite the absence of cells. Differences in storage moduli indicate there was some gel degradation, which may be due to potential MMPs present in the serum. However, the wet and dry mass were comparable between the degradable groups on day 7, demonstrating the gels remained intact. Taken together, these data suggest that some hydrogel degradation occurred but not to the level where the overall structural integrity of the gel was jeopardized, evidenced by the lack of changes in the wet and dry mass. To evaluate cell-mediated degradation of the PEG gels, we incorporated EC-MSC spheroids and analyzed degradation *via* rheology and wet/dry mass. There was a noticeable decrease in storage moduli by day 1 for fully and partially degradable gels, which was more pronounced by day 7. The decrease in wet and dry mass of GPQ-A crosslinked gels compared to GPQ-A:PEG-DT and PEG-DT gels further supported these data, demonstrating that we can successfully modulate the rate of degradation of these hydrogels. Overall, degradation was more prominent in cell-laden gels, indicating that cells were degrading the material *via* enzymatic cleavage. MMP-2 secretion correlated with increasing GPQ-A concentration, suggesting there may be a positive feedback loop between MMP-2 secretion levels and the degree of gel degradation [49]. Indeed, we previously observed increases in MMP-2 gene expression in DRG neurons entrapped in fibrin gels with increasing stiffness, yet the relationship between stiffness and degradation was not evaluated [50]. These data suggest that entrapped cells are responsive to changes in void volume and perhaps ligand availability made possible by degradation. In addition, cells are responsive to scaffold pore diameter and mesh size [51,52], which warrants further investigation to elucidate the crosstalk between scaffold structure and EC-MSC spheroid behavior (*e.g.*, secretory potential, cell migration).

A key finding of this work is that gel degradation is critical for cellular proliferation and significantly influences metabolic activity using co-culture spheroids. Over 7 days, DNA content increased, regardless of gel formulation, emphasizing the cytocompatibility of PEG-4MAL and the benefits of using PEG-4MAL as our choice of platform to interrogate the role of gel degradation. When treated with GM6001, spheroids in all groups exhibited impaired proliferation. Metabolic activity was also influenced by gel degradation. Metabolic activity on day 1 was not significantly different between the degradable groups but by day 7, only the groups with GPQ-A supported increases in metabolic activity while non-degradable counterparts showed a decrease.

Degradable scaffolds influence the MSC secretome (*e.g.*, MMP-2, IL-10, SDF-1 secretion), collagen deposition, migration, and neovascularization [53,54]. However, the influence of degradation rate on modulating cell behavior is not well characterized. Our study demonstrates that the degree of matrix degradability significantly influenced cellular sprouting, spheroid secretome, and expression of angiogenesis-related genes. On day 7, fully, partially, and non-degradable gels facilitated the longest, intermediate, and shortest average sprout length, respectively. Future investigation is merited to determine cell outgrowth alignment from the spheroids as a potential stimulus to accelerate neovascularization and wound healing. We further observed robust F-actin structure, signifying cell elongation and protrusion in degradable gels. Using a multiplex cytokine assay, we characterized the unique profile compositions of the spheroid secretome when entrapped in different gel formulations. Spheroids in gels with greater degradability exhibited increased secretion of proangiogenic factors (*i.e.*, VEGF, HGF). Based on the correlations between matrix degradability with cell sprouting/migration and secretion of proangiogenic cytokines, we interrogated the interplay of sprouting/migration and proangiogenic potential of EC-MSC spheroids by inhibiting migration (LatA) and matrix degradation (GM6001). Cells in LatA- and GM6001-treated degradable gels had reduced VEGF and HGF secretion comparable to spheroids in non-degradable PEG-DT gels. Total VEGF and HGF was significantly reduced in GPQ-A versus GPQ-A:PEG-DT gels. We further expected cells in treated degradable gels to exhibit *VEGF* and *HGF* expression levels similar to LatA-treated non-degradable gels, regardless of RGD modification. Intriguingly, while inhibiting migration and degradation in GPQ-A and GPQ-A:PEG-DT resulted in gene expressions similar to PEG-DT gels, spheroids in gels without RGD motifs had consistently lower *VEGF* and *HGF* expression, although not significant. This suggests that cell adhesion, in addition to cell migration and matrix degradation, contributes to the expression of angiogenesis-related genes. We observed similar findings when MSC spheroids were entrapped in RGD-modified alginate hydrogels [55]. This phenomenon merits further investigation to elucidate the interplay of cell adhesion, cell migration, and matrix degradation.

We used a full-thickness *ex vivo* skin model as a controlled environment to study the effects of our degradable and non-degradable gels without other confounding factors associated with wound healing commonly observed in animal models. However, fully degradable gels survived only 5 days in the defect, limiting their translational potential and ability to compare to the other groups. Full-thickness models contain epidermal and dermal layers with skin structures and appendages (*e.g.*, rete ridges and hair follicles) that play a critical role in native skin regeneration that are lost in partial thickness models. This *ex vivo* skin model allowed us to study regeneration in the presence of an active stem cell population. We chose day 7 as an experimental endpoint to evaluate epithelialization, cell migration, and keratinocyte proliferation during the onset of the proliferation stage where the effects of the secretory profiles of spheroids would be of higher impact on skin regeneration [56,57].

Our data suggest that partially degradable gels enhanced re-epithelialization of the wound site compared to the non-treated control as demonstrated by the regeneration of the epidermal layer. Although non-degradable gels also showed improved epithelialization compared to the non-treated control, we observed a higher occurrence of epidermal detachment across the samples and smaller epidermal thickness at day 7 compared to the wounds treated with the degradable gels. The observation of more CK14+ cells in wounds treated with degradable constructs compared to those treated with non-degradable gels indicates the presence of a proliferative basal keratinocyte population which is critical to restoring epidermal stratification and suggests early signs of restoration of barrier function. Interestingly, there were no distinct changes in COL1 expression between degradable and non-degradable groups on day 7. The presence of COL1 in the upper dermal layer may suggest that although keratinocyte proliferation has initiated epidermal stratification, dermal fibroblasts remained on the upper epidermal layer and continued producing COL1. Future studies in a full-thickness *in vivo* model would enable interrogation of the mechanistic contributions from the immune response or circulating ECs.

Additionally, increasing the experimental time frame from 7 to 14 days to study wound progression at several time points would further reveal the synergistic effects of gel degradation, growth factor secretion, and MMPs secretion on wound closure and epithelialization. Furthermore, future work is necessary to explore the application of this platform to fill and treat irregularly shaped wounds with variable severities.

5. Conclusion

We engineered hydrogels with tunable degradation to investigate the role of microenvironmental remodeling on the therapeutic potential of EC-MSC spheroids. This study highlights the importance of matrix remodeling on modulating cellular behaviors essential for tissue regeneration (*i.e.*, proliferation, migration, proangiogenic potential). For the first time, EC-MSC spheroids are leveraged in a degradable hydrogel to stimulate wound healing in a clinically relevant full-thickness *ex vivo* skin burn model. Collectively, matrix remodeling is essential and should be carefully considered when choosing an environment to use as a carrier for wound healing.

Credit author statement

Victoria L. Thai: conception and design, financial support, collection and/or assembly of data, data analysis and interpretation, manuscript writing, and final approval of manuscript; David H. Ramos-Rodriguez: conception and design, financial support, collection and/or assembly of data, data analysis and interpretation, manuscript writing, and final approval of manuscript; Meron Mesfin: collection and/or assembly of data, and final approval of manuscript; J. Kent Leach: conception and design, financial support, data analysis and interpretation, manuscript writing, and final approval of manuscript.

Declaration of competing interest

The authors declare the following financial interests/personal relationships which may be considered as potential competing interests. Kent Leach reports financial support was provided by National Institutes of Health. Kent Leach reports a relationship with Journal of Biomedical Materials Research Part A that includes: board membership.

Data availability

Data will be made available on request.

Acknowledgements

This work was supported by the National Institutes of Health (R01 DE025899, R01 AR079211); the NHLBI Training Program in Basic and Translational Cardiovascular Science at UC Davis (T32 HL086350); the California Institute of Regenerative Medicine (CIRM) training program (grant number ECUC4-12792 (CIRM EDUC4 Research Training Program)). JKL gratefully acknowledges financial support from the Lawrence J. Ellison Endowed Chair of Musculoskeletal Research. Figs. 1A and 6A were created with Biorender.com. The content is solely the responsibility of the authors and does not necessarily represent the official views of the National Institutes of Health.

Appendix A. Supplementary data

Supplementary data to this article can be found online at https://doi.org/10.1016/j.mtbio.2023.100769.

APPENDICES.

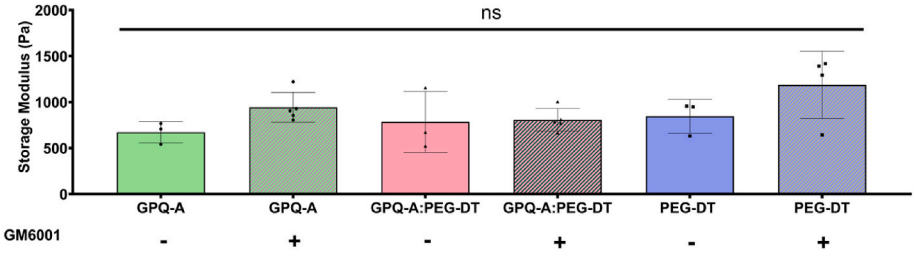

Fig. A.1. GM6001 treatment did not affect the storage modulus of acellular PEG gels after one day (n = 3–5).

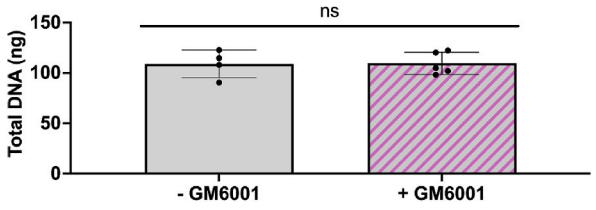

Fig. A.2. GM6001 treatment had no effect on proliferation in EC-MSC spheroids after 7 days (n = 4–5).

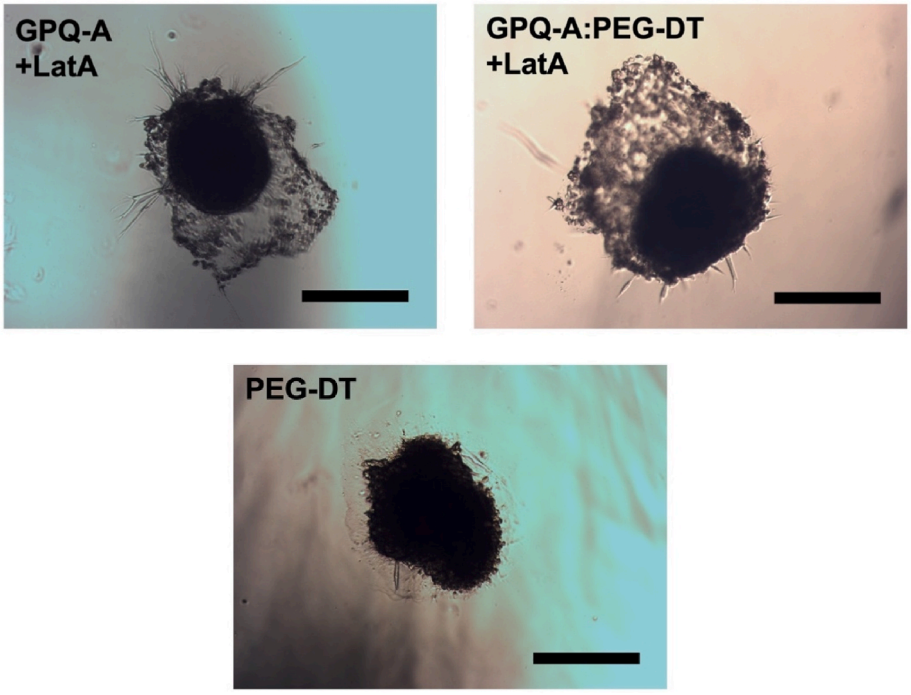

Fig. A.3. LatA treatment (0.1 μM) inhibited some but not all cell migration in GPQ-A and GPQ-A:PEG-DT gels by day 7. Scale bars are 500 μm.

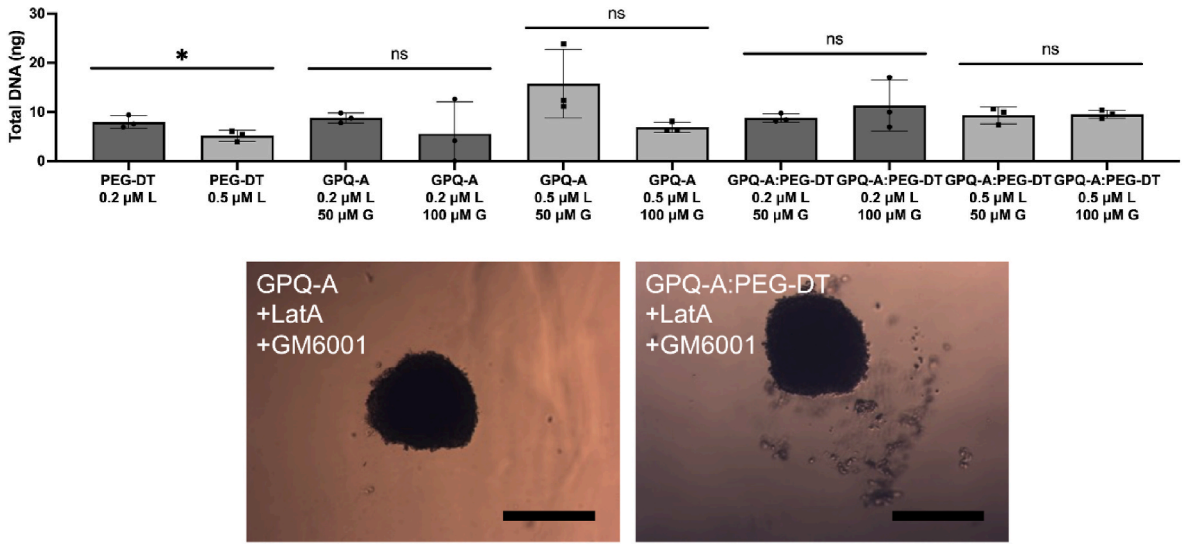

Fig. A.4. Treatment with 0.2 μM LatA and 50 μM GM6001 inhibited cellular migration (observed in brightfield images) and facilitated similar levels of cellular proliferation in degradable hydrogels compared to non-degradable hydrogels based on total DNA content following 7 days of culture ($n = 3$). PEG-DT groups treated with higher concentrations of LatA resulted in reduced DNA content. Significance is denoted by asterisks where * ($p \leq 0.05$). Scale bars are 500 μm. Abbreviations: L – LatA; G – GM6001.

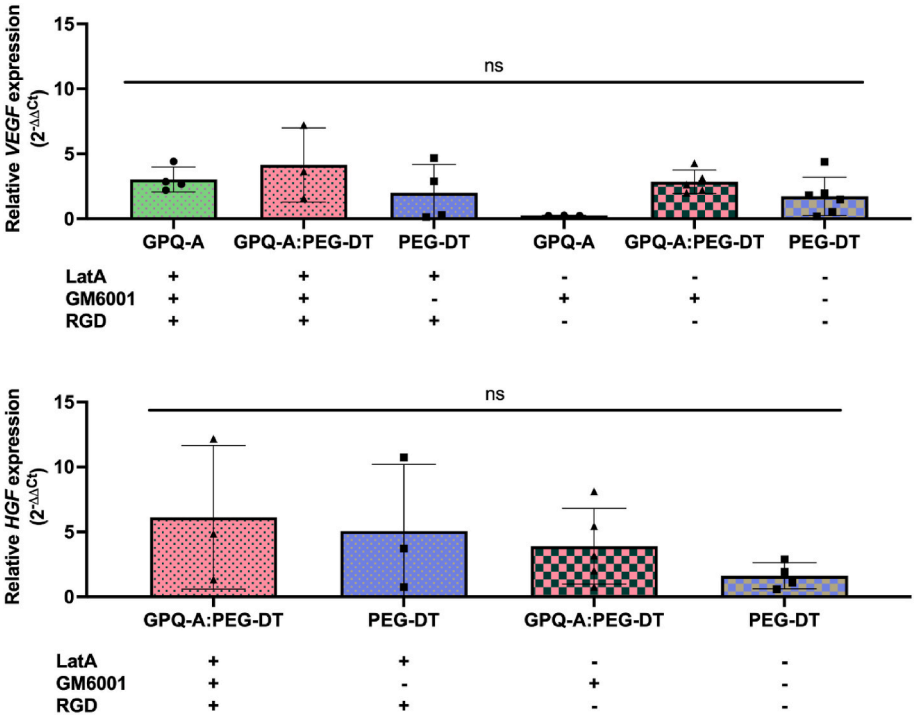

Fig. A.5. Relative gene expression of *VEGF* and *HGF* by EC-MSC spheroids treated with 0.2 μM LatA and 50 μM GM6001 demonstrate *VEGF* and *HGF* expression are dependent on hydrogel degradation (n = 3–6).

References

[1] E. Everett, N. Mathioudakis, Update on management of diabetic foot ulcers, Ann. N. Y. Acad. Sci. 1411 (1) (2018) 153–165.

[2] N.B. Menke, K.R. Ward, T.M. Witten, D.G. Bonchev, R.F. Diegelmann, Impaired wound healing, Clin. Dermatol. 25 (1) (2007) 19–25.

[3] K. Jarbrink, G. Ni, H. Sonnergren, A. Schmidtchen, C. Pang, R. Bajpai, J. Car, Prevalence and incidence of chronic wounds and related complications: a protocol for a systematic review, Syst. Rev. 5 (1) (2016) 152.

[4] C.K. Sen, Human wound and its burden: updated 2020 compendium of estimates, Adv. Wound Care 10 (5) (2021) 281–292.

[5] C.N. Tchanque-Fossuo, S.E. Dahle, H. Lev-Tov, K.I.M. West, C.S. Li, D.M. Rocke, R. R. Isseroff, Cellular versus acellular matrix devices in the treatment of diabetic foot ulcers: interim results of a comparative efficacy randomized controlled trial, J. Tissue Eng. Regen. Med. 13 (8) (2019) 1430–1437.

[6] S.R. Park, J.W. Kim, H.S. Jun, J.Y. Roh, H.Y. Lee, I.S. Hong, Stem cell secretome and its effect on cellular mechanisms relevant to wound healing, Mol. Ther. 26 (2) (2018) 606–617.

[7] R. Tiruvannamalai Annamalai, A.Y. Rioja, A.J. Putnam, J.P. Stegemann, Vascular network formation by human microvascular endothelial cells in modular fibrin microtissues, ACS Biomater. Sci. Eng. 2 (11) (2016) 1914–1925.

[8] D. Jiang, Y. Qi, N.G. Walker, A. Sindrilaru, A. Hainzl, M. Wlaschek, S. MacNeil, K. Scharffetter-Kochanek, The effect of adipose tissue derived MSCs delivered by a chemically defined carrier on full-thickness cutaneous wound healing, Biomaterials 34 (10) (2013) 2501–2515.

[9] L. Chen, E.E. Tredget, P.Y. Wu, Y. Wu, Paracrine factors of mesenchymal stem cells recruit macrophages and endothelial lineage cells and enhance wound healing, PLoS One 3 (4) (2008), e1886.

[10] K.H. Griffin, S.W. Fok, J.K. Leach, Strategies to capitalize on cell spheroid therapeutic potential for tissue repair and disease modeling, NPJ Reg. Med. 7 (1) (2022) 70.

[11] S.H. Bhang, S.W. Cho, W.G. La, T.J. Lee, H.S. Yang, A.Y. Sun, S.H. Baek, J.W. Rhie, B.S. Kim, Angiogenesis in ischemic tissue produced by spheroid grafting of human adipose-derived stromal cells, Biomaterials 32 (11) (2011) 2734–2747.

[12] T.T. Chang, M. Hughes-Fulford, Monolayer and spheroid culture of human liver hepatocellular carcinoma cell line cells demonstrate distinct global gene expression patterns and functional phenotypes, Tissue Eng. Part A 15 (3) (2009) 559–567.

[13] A. Jaukovic, D. Abadjieva, D. Trivanovic, E. Stoyanova, M. Kostadinova, S. Pashova, S. Kestendjieva, T. Kukolj, M. Jeseta, E. Kistanova, M. Mourdjeva, Specificity of 3D MSC spheroids microenvironment: impact on MSC behavior and properties, Stem. Cell Rev. Rep. 16 (5) (2020) 853–875.

[14] C.E. Vorwald, S. Joshee, J.K. Leach, Spatial localization of endothelial cells in heterotypic spheroids influences notch signaling, J. Mol. Med. (Berl.) 98 (3) (2020) 425–435.

[15] V.L. Thai, D.O. Candelas, J.K. Leach, Tuning the microenvironment to create functionally distinct mesenchymal stromal cell spheroids, Ann. Biomed. Eng. 51 (7) (2023) 1558–1573.

[16] S.H. Hsu, T.T. Ho, N.C. Huang, C.L. Yao, L.H. Peng, N.T. Dai, Substrate-dependent modulation of 3D spheroid morphology self-assembled in mesenchymal stem cell-endothelial progenitor cell coculture, Biomaterials 35 (26) (2014) 7295–7307.

[17] M.P. Caley, V.L. Martins, E.A. O'Toole, Metalloproteinases and wound healing, Adv. Wound Care 4 (4) (2015) 225–234.

[18] S. Guo, L.A. Dipietro, Factors affecting wound healing, J. Dent. Res. 89 (3) (2010) 219–229.

[19] S. Hauck, P. Zager, N. Halfter, E. Wandel, M. Torregrossa, A. Kakpenova, S. Rother, M. Ordieres, S. Rathel, A. Berg, S. Moller, M. Schnabelrauch, J.C. Simon, V. Hintze, S. Franz, Collagen/hyaluronan based hydrogels releasing sulfated hyaluronan improve dermal wound healing in diabetic mice via reducing inflammatory macrophage activity, Bioact. Mater. 6 (12) (2021) 4342–4359.

[20] Y. You, K. Kobayashi, B. Colak, P. Luo, E. Cozens, L. Fields, K. Suzuki, J. Gautrot, Engineered cell-degradable poly(2-alkyl-2-oxazoline) hydrogel for epicardial placement of mesenchymal stem cells for myocardial repair, Biomaterials 269 (2021), 120356.

[21] J. Dai, W. Qiao, J. Shi, C. Liu, X. Hu, N. Dong, Modifying decellularized aortic valve scaffolds with stromal cell-derived factor-1alpha loaded proteolytically degradable hydrogel for recellularization and remodeling, Acta Biomater. 88 (2019) 280–292.

[22] E.A. Phelps, N.O. Enemchukwu, V.F. Fiore, J.C. Sy, N. Murthy, T.A. Sulchek, T. H. Barker, A.J. Garcia, Maleimide cross-linked bioactive PEG hydrogel exhibits improved reaction kinetics and cross-linking for cell encapsulation and in situ delivery, Adv. Mater. 24 (1) (2012) 64–70, 2.

[23] A.Y. Clark, K.E. Martin, J.R. Garcia, C.T. Johnson, H.S. Theriault, W.M. Han, D. W. Zhou, E.A. Botchwey, A.J. Garcia, Integrin-specific hydrogels modulate transplanted human bone marrow-derived mesenchymal stem cell survival, engraftment, and reparative activities, Nat. Commun. 11 (1) (2020) 114.

[24] A.D. Shubin, T.J. Felong, B.E. Schutrum, D.S.L. Joe, C.E. Ovitt, D.S.W. Benoit, Encapsulation of primary salivary gland cells in enzymatically degradable poly (ethylene glycol) hydrogels promotes acinar cell characteristics, Acta Biomater. 50 (2017) 437–449.

[25] J.J. Moon, J.E. Saik, R.A. Poche, J.E. Leslie-Barbick, S.H. Lee, A.A. Smith, M. E. Dickinson, J.L. West, Biomimetic hydrogels with pro-angiogenic properties, Biomaterials 31 (14) (2010) 3840–3847.

[26] J. Li, D.J. Mooney, Designing hydrogels for controlled drug delivery, Nat. Rev. Mater. 1 (12) (2016).

[27] S. Liu, H. Cao, R. Guo, H. Li, C. Lu, G. Yang, J. Nie, F. Wang, N. Dong, J. Shi, F. Shi, Effects of the proportion of two different cross-linkers on the material and biological properties of enzymatically degradable PEG hydrogels, Polym. Degrad. Stabil. 172 (2020), 109067.

[28] E.A. Phelps, D.M. Headen, W.R. Taylor, P.M. Thule, A.J. Garcia, Vasculogenic bio-synthetic hydrogel for enhancement of pancreatic islet engraftment and function in type 1 diabetes, Biomaterials 34 (19) (2013) 4602–4611.

[29] A.J. Garcia, PEG-maleimide hydrogels for protein and cell delivery in regenerative medicine, Ann. Biomed. Eng. 42 (2) (2014) 312–322.
[30] L.E. Mead, D. Prater, M.C. Yoder, D.A. Ingram, Isolation and characterization of endothelial progenitor cells from human blood, Curr. Protoc. Stem Cell Biol. Chapter 2 (2008). Unit 2C 1.
[31] C.E. Vorwald, S.S. Ho, J. Whitehead, J.K. Leach, High-throughput formation of mesenchymal stem cell spheroids and entrapment in alginate hydrogels, Methods Mol. Biol. 1758 (2018) 139–149.
[32] C.E. Vorwald, K.C. Murphy, J.K. Leach, Restoring vasculogenic potential of endothelial cells from diabetic patients through spheroid formation, Cell. Mol. Bioeng. 11 (4) (2018) 267–278.
[33] R. Cruz-Acuna, M. Quiros, S. Huang, D. Siuda, J.R. Spence, A. Nusrat, A.J. Garcia, PEG-4MAL hydrogels for human organoid generation, culture, and in vivo delivery, Nat. Protoc. 13 (9) (2018) 2102–2119.
[34] T.P. Kraehenbuehl, P. Zammaretti, A.J. Van der Vlies, R.G. Schoenmakers, M. P. Lutolf, M.E. Jaconi, J.A. Hubbell, Three-dimensional extracellular matrix-directed cardioprogenitor differentiation: systematic modulation of a synthetic cell-responsive PEG-hydrogel, Biomaterials 29 (18) (2008) 2757–2766.
[35] T.E.G. Krueger, D.L.J. Thorek, S.R. Denmeade, J.T. Isaacs, W.N. Brennen, Concise review: mesenchymal stem cell-based drug delivery: the good, the bad, the ugly, and the promise, Stem Cells Transl. Med.. 7 (9) (2018) 651–663.
[36] R.H. Adamson, Microvascular endothelial cell shape and size in situ, Microvasc. Res. 46 (1) (1993) 77–88.
[37] M. Kim, M. Hong, J. Kim, H. Kim, S.J. Lee, S. Goo Kang, D. Jae Cho, Bovine follicular fluid and serum share a unique isoform of matrix metalloproteinase-2 that is degraded by the oviductal fluid, Biol. Reprod. 65 (6) (2001) 1726–1731.
[38] N.O. Enemchukwu, R. Cruz-Acuna, T. Bongiorno, C.T. Johnson, J.R. Garcia, T. Sulchek, A.J. Garcia, Synthetic matrices reveal contributions of ecm biophysical and biochemical properties to epithelial morphogenesis, J. Cell Biol. 212 (1) (2016) 113–124.
[39] S. Neuss, E. Becher, M. Woltje, L. Tietze, W. Jahnen-Dechent, Functional expression of hgf and hgf receptor/c-met in adult human mesenchymal stem cells suggests a role in cell mobilization, tissue repair, and wound healing, Stem Cell. 22 (3) (2004) 405–414.
[40] L.J. Stevens, A. Page-McCaw, A secreted MMP is required for reepithelialization during wound healing, Mol. Biol. Cell 23 (6) (2012) 1068–1079.
[41] S.A. Castleberry, B.D. Almquist, W. Li, T. Reis, J. Chow, S. Mayner, P.T. Hammond, Self-assembled wound dressings silence MMP-9 and improve diabetic wound healing in vivo, Adv. Mater. 28 (9) (2016) 1809–1817.
[42] D.G. Armstrong, E.B. Jude, The role of matrix metalloproteinases in wound healing, J. Am. Podiatr. Med. Assoc. 92 (1) (2002) 12–18.
[43] S. Wangler, A. Kamali, C. Wapp, K. Wuertz-Kozak, S. Hackel, C. Fortes, L. M. Benneker, L. Haglund, R.G. Richards, M. Alini, M. Peroglio, S. Grad, Uncovering the secretome of mesenchymal stromal cells exposed to healthy, traumatic, and degenerative intervertebral discs: a proteomic analysis, Stem Cell Res. Ther. 12 (1) (2021) 11.
[44] A. Lueckgen, D.S. Garske, A. Ellinghaus, R.M. Desai, A.G. Stafford, D.J. Mooney, G. N. Duda, A. Cipitria, Hydrolytically-degradable click-crosslinked alginate hydrogels, Biomaterials 181 (2018) 189–198.
[45] A. Lueckgen, D.S. Garske, A. Ellinghaus, D.J. Mooney, G.N. Duda, A. Cipitria, Enzymatically-degradable alginate hydrogels promote cell spreading and in vivo tissue infiltration, Biomaterials 217 (2019), 119294.
[46] J.R. Martin, P. Patil, F. Yu, M.K. Gupta, C.L. Duvall, Enhanced stem cell retention and antioxidative protection with injectable, ROS-degradable PEG hydrogels, Biomaterials 263 (2020), 120377.
[47] P.M. Kharkar, K.L. Kiick, A.M. Kloxin, Designing degradable hydrogels for orthogonal control of cell microenvironments, Chem. Soc. Rev. 42 (17) (2013) 7335–7372.
[48] K.E. Martin, M.D. Hunckler, E. Chee, J.D. Caplin, G.F. Barber, P.P. Kalelkar, R. S. Schneider, A.J. García, Hydrolytic hydrogels tune mesenchymal stem cell persistence and immunomodulation for enhanced diabetic cutaneous wound healing, Biomaterials (2023), 122256.
[49] A. Rastogi, H. Kim, J.D. Twomey, A.H. Hsieh, MMP-2 mediates local degradation and remodeling of collagen by annulus fibrosus cells of the intervertebral disc, Arthritis Res. Ther. 15 (2) (2013) R57.
[50] A.J. Man, H.E. Davis, A. Itoh, J.K. Leach, P. Bannerman, Neurite outgrowth in fibrin gels is regulated by substrate stiffness, Tissue Eng. 17 (23–24) (2011) 2931–2942.
[51] T.H. Qazi, D.J. Mooney, G.N. Duda, S. Geissler, Biomaterials that promote cell-cell interactions enhance the paracrine function of MSCs, Biomaterials 140 (2017) 103–114.
[52] W.B. Swanson, M. Omi, Z. Zhang, H.K. Nam, Y. Jung, G. Wang, P.X. Ma, N. E. Hatch, Y. Mishina, Macropore design of tissue engineering scaffolds regulates mesenchymal stem cell differentiation fate, Biomaterials 272 (2021), 120769.
[53] J.A. Zullo, E.P. Nadel, M.M. Rabadi, M.J. Baskind, M.A. Rajdev, C.M. Demaree, R. Vasko, S.S. Chugh, R. Lamba, M.S. Goligorsky, B.B. Ratliff, The secretome of hydrogel-coembedded endothelial progenitor cells and mesenchymal stem cells instructs macrophage polarization in endotoxemia, Stem Cells Transl. Med. 4 (7) (2015) 852–861.
[54] K. Shoma Suresh, S. Bhat, B.R. Guru, M.S. Muttigi, R.N. Seetharam, A nanocomposite hydrogel delivery system for mesenchymal stromal cell secretome, Stem Cell Res. Ther. 11 (1) (2020) 205.
[55] S.S. Ho, K.C. Murphy, B.Y. Binder, C.B. Vissers, J.K. Leach, Increased survival and function of mesenchymal stem cell spheroids entrapped in instructive alginate hydrogels, Stem Cells Transl. Med. 5 (6) (2016) 773–781.
[56] M.J. Blair, J.D. Jones, A.E. Woessner, K.P. Quinn, Skin structure-function relationships and the wound healing response to intrinsic aging, Adv. Wound Care 9 (3) (2020) 127–143.
[57] M. Damen, L. Wirtz, E. Soroka, H. Khatif, C. Kukat, B.D. Simons, H. Bazzi, High proliferation and delamination during skin epidermal stratification, Nat. Commun. 12 (1) (2021) 3227.